

DMD #44644

**Time-Dependent Inhibition and Estimation of CYP3A Clinical
Pharmacokinetic Drug-Drug Interactions Using Plated Human Cell Systems**

Daniel R. Albaugh, Cody L. Fullenwider, Michael B. Fisher, and J. Matthew Hutzler

Medicinal Chemistry (Drug Metabolism and Pharmacokinetics, DMPK),

Boehringer-Ingelheim Pharmaceuticals Inc.,

Ridgefield, Connecticut (D.R.A., C.L.F., J.M.H.); and

ProPharma Services, Oxford, Connecticut (M.B.F)

DMD #44644

Running Title: Time-Dependent Inhibition Using Plated Human Cell Systems

Address Correspondence to:

Daniel R. Albaugh

Boehringer-Ingelheim Pharmaceuticals Inc., Translational Research (DMPK)

175 Briar Ridge Road, R&D 10574, Ridgefield, CT 06877

Tel: 203-791-6358

Fax: 203-791-6130

Email: daniel.albaugh@Boehringer-Ingelheim.com

Text Pages: 27

Tables: 3

Figures: 8

References: 36

Words in Abstract: 246

Words in Introduction: 466

Words in Discussion: 1062

Non-Standard Abbreviations:

TDI, time-dependent inhibition; P450, cytochrome P450; DDI, drug-drug interaction; HLM, human liver microsome; time-dependent; HPLC, high-performance liquid chromatograph; LC/MS/MS, liquid chromatography tandem mass spectrometry; AUC, area under the curve.

Abstract

The current studies assessed the utility of freshly plated hepatocytes, cryopreserved plated hepatocytes, and cryopreserved plated HepaRG cells for the estimation of inactivation parameters k_{inact} and K_I for CYP3A. This was achieved using a subset of CYP3A time-dependent inhibitors (fluoxetine, verapamil, clarithromycin, troleandomycin, and mibefradil) representing a range of potencies. The estimated k_{inact} and K_I values for each time-dependent inhibitor were compared to those obtained using human liver microsomes, and used to estimate the magnitude of clinical pharmacokinetic DDI. The inactivation kinetic parameter, k_{inact} was most consistent across systems tested for clarithromycin, verapamil, and troleandomycin, with a high k_{inact} of 0.91 min^{-1} observed for mibefradil in HepaRG cells. The apparent K_I estimates derived from the various systems displayed a range of variability from 3-fold for clarithromycin ($5.4\text{-}17.7 \mu\text{M}$) up to 6-fold for verapamil ($1.9\text{-}12.6 \mu\text{M}$). In general, the inactivation kinetic parameters derived from the cell systems tested fairly replicated what was observed in TDI studies using HLMs. Despite some of the observed differences in inactivation kinetic parameters, the estimated DDIs derived from each of the tested systems generally agreed with the clinically reported DDI within approximately 2-fold. In addition, a plated cell approach offered the ability to conduct longer primary incubations (greater than 30 minutes), which afforded improved ability to identify the weak time-dependent inhibitor fluoxetine. Overall, results from these studies suggest that in vitro inactivation parameters generated from plated cell systems may be a practical approach for identifying time-dependent inhibitors, and estimating the magnitude of clinical DDIs.

INTRODUCTION

Time-dependent inhibition (TDI) of cytochrome P450 enzymes is a major concern due to the potential for clinically significant drug-drug interactions (DDI) (Lin and Lu, 1998). Therefore, from a drug discovery perspective it is critical to not just qualitatively identify, but also to quantitatively estimate the magnitude of any potential interaction for new chemical entities prior to preclinical development (Mayhew et al., 2000).

Typically, kinetic parameters of enzyme inactivation (k_{inact} and K_I) are measured in a two-staged assay with multiple concentrations and time points using human liver microsomes (HLMs) (Jones et al., 1999; Grimm et al., 2009). The process of using in vitro inactivation data to estimate and rank order the DDI potential of compounds is well established (Mayhew et al., 2000; Obach et al., 2006; Obach et al., 2007), where the in vitro inactivation kinetic parameters along with the in vivo systemic and intestinal concentration of the time-dependent inhibitor, fraction metabolized and intestinal extraction ratio of the victim probe drug, and enzyme degradation rates (Correia, 1991; Greenblatt et al., 2003; Ghanbari et al., 2006) are used to estimate the potential for a clinical DDI (Obach et al., 2006; Obach et al., 2007). However, precipitants of TDI are not always products of oxidative metabolism (Ogilvie et al., 2006; Baer et al., 2009; Xu et al., 2009; Honkalammi et al., 2011) and therefore it may be more relevant to assess TDI in a system containing the full complement of drug-metabolizing enzymes, such as hepatocytes (Li, 1997; Zhao et al., 2005; Zhao, 2008; Li and Doshi, 2011).

Many investigators have evaluated the use of hepatocyte suspensions (Zhao et al., 2005; McGinnity et al., 2006; Van et al., 2007; Zhao et al., 2007; Lu et al., 2008a; Lu et al., 2008b; Baer et al., 2009; Mao et al., 2011) for time-dependent inhibition studies. Certainly the use of hepatocytes for time-dependent inhibition holds distinct advantages over the use of microsomes,

DMD #44644

including being more physiologically relevant and offering the ability to conduct longer incubations. However, there are some potential difficulties associated with time-dependent inhibition studies using hepatocyte suspensions, including removal of time-dependent inhibitor while maintaining cell viability (Zhao, 2008).

The objective of the current studies were to investigate fresh plated primary hepatocytes, cryopreserved plated hepatocytes, and cryopreserved HepaRG plated cell systems for their ability to generate in vitro inactivation parameters comparable to those generated using HLMs. The k_{inact} and K_I values obtained in the plated cell systems and human liver microsomes were used to predict clinical pharmacokinetic DDIs and then compared to the observed clinical drug interaction. The plated methods utilized to conduct the time-dependent inhibition experiments overcome many of the limitations of a hepatocyte suspension assay. The advantages, disadvantages, and ability to quantitatively predict clinical pharmacokinetic DDI for each of the tested systems, as compared to the commonly employed TDI assay in HLMs, are discussed.

Materials and Methods

Chemicals. Clarithromycin, mibefradil, verapamil, troleandomycin, and fluoxetine (Figure 1), acetonitrile with 0.1% formic acid, water with 0.1% formic acid, 1.0 M monobasic potassium phosphate solution, and 1.0 M dibasic potassium phosphate solution were purchased from Sigma-Aldrich (St. Louis, MO). Midazolam and α -hydroxymidazolam-d4 were obtained from Cerilliant Corporation (Round Rock, TX). NADPH was obtained from EMD (Gibbstown, NJ). Primary plated human hepatocytes isolated from a 55 year old male Caucasian (donor H1014) were obtained in a 24 well format from XenoTech (Lenexa, Kansas). Plateable inducible cryopreserved human hepatocytes, lot 4205, isolated from a 42 year old male Caucasian, HepaRG™ cells, Williams E medium, collagen coated 24 well plates, matrigel, cryopreserved hepatocyte recovery medium (CHRM), primary hepatocyte thawing, plating and maintenance supplements, GlutaMAX, HepaRG™ thawing, plating and general purpose medium supplement were acquired from Life Technologies Inc. (Carlsbad, CA). Human liver microsomes (BD Ultra pool 150) were purchased from BD Biosciences (Bedford, MA). All other reagents were of the highest purity available.

TDI in Human Liver Microsomes. Incubations were performed in an automated fashion using a Tecan Evo (Durham, NC) in polypropylene tubes containing 100 mM phosphate buffer, pH 7.4, 0.1 mg/mL human liver microsomes, and 1 mM NADPH at 37 °C (primary incubation). Final test compound concentrations were as follows: fluoxetine and clarithromycin (0 to 50 μ M), mibefradil (0 to 7.5 μ M), TAO (0 to 5 μ M) and verapamil (0 to 25 μ M). After initiation of the primary incubation by the addition of NADPH, samples (10 μ L) were taken at 0, 1, 3, 5, 15 and 30 minutes and added to a secondary incubation consisting of 190 μ L phosphate buffer containing 15 μ M midazolam (saturating concentration) and 1 mM NADPH. The secondary reactions were quenched

DMD #44644

after 8 minutes using one volume of ice-cold acetonitrile containing α -hydroxymidazolam-d4 (100 nM) and centrifuged at 3000 x g for 10 minutes. Supernatants were transferred to a 96 well plate and analyzed by LC/MS/MS.

Cell Culture. Upon receipt of plated primary human hepatocytes, cells were washed and incubated for 48 hours with daily media changes using hepatocyte maintenance media. Plateable inducible cryopreserved human hepatocytes were thawed for two minutes at 37° C and resuspended in prewarmed CHRM® media. Resuspended cells were centrifuged at 100 x g for 10 minutes. Supernatant was removed and hepatocyte maintenance media was added to achieve a final cell density of 8.0×10^5 viable cells/mL. Cell viability was assessed by trypan blue exclusion and was greater than 70 percent. Collagen coated 24 well plates were seeded at a density of 4.0×10^5 cells/well. Plates were incubated for six hours in a humidified incubator at 37° C, 5% CO₂. After incubation, media was replaced with fresh ice cold hepatocyte maintenance media containing 0.35 mg/mL Geltrex™ and incubated overnight.

HepaRG™ cells were thawed for two minutes at 37° C and resuspended in 50 mL prewarmed media consisting of Williams E media with 1% GlutaMAX™ and HepaRG™ thawing supplement. Resuspended cells were centrifuged at 360 x g for 4 minutes. Supernatant was removed and HepaRG™ plating media consisting of Williams E Media with 1% GlutaMAX™ and HepaRG™ plating supplement was added to achieve a final cell density of 6.0×10^5 viable cells/mL. Cell viability was assessed by trypan blue exclusion and was greater than 70 percent. Collagen coated 24 well plates were seeded at a density of 3.0×10^5 cells/well and cultured in a humidified incubator at 37° C, 5% CO₂ for 4 hours.

TDI in Plated Cells. Incubations were performed in a humidified incubator at 37°C, 5% CO₂. Williams E Media was removed from each collagen coated 24-well plate by vacuum aspiration and

DMD #44644

replaced with 0.5 mL of Williams E Media containing time-dependent inhibitor to initiate the primary incubation. Williams E Media containing time-dependent inhibitor was removed by vacuum aspiration at 0, 5, 15, and 30 minutes (0, 15, 45, and 90 minutes for fluoxetine). Cells were washed with 0.5 mL of Williams E Media and removed using vacuum aspiration prior to the addition of 0.5 mL of Williams E Media containing 15 μ M midazolam to initiate the secondary incubation. 100 μ L of incubate was removed after an 8 minute secondary incubation and the reaction was immediately terminated by flash freezing in a dry ice/methanol bath. After flash freezing the samples, 0.3 mL of ice-cold acetonitrile containing α -hydroxymidazolam-d4 (100 nM) was added. Samples were centrifuged at 3000 x g for 10 minutes. Supernatant was transferred to a 96 well plate and analyzed by LC/MS/MS.

LC/MS/MS Analysis. Quantitation of 1'-hydroxy midazolam (MRM 342>203) was performed using an AB Sciex API-5000 triple quadrupole mass spectrometer (Foster City, CA) equipped with an electrospray ionization (ESI) interface in positive ion mode and connected in-line to a Waters Acquity UPLC system (Milford, MA). Separation of 1'-hydroxy midazolam was performed using a Waters Acquity BEH C8 1.7 μ m (2.1 x 50 mm) column maintained at 50°C. The mobile phase flow rate was 0.5 mL/min. Initial conditions were 55%A (0.1% formic acid in water) and 45%B (0.1% formic acid in acetonitrile). Initial conditions were held for 0.5 minutes, followed by a linear gradient to 90% B over 0.05 minutes (hold for 0.25 minutes), and then re-equilibration to initial conditions with a total analytical run time of 1.0 minutes.

Data Analysis. Peak areas for 1'-hydroxy midazolam and α -hydroxymidazolam-d4 were determined using Analyst software (Version 1.4.2; AB Sciex, Foster City, CA). Analyte/IS peak area ratios were used to calculate percent activity remaining based on comparison with time zero samples. The apparent inactivation rate (k_{obs}) for each time-dependent inhibitor concentration

DMD #44644

were determined from plots of the natural logarithm of percent activity remaining and primary incubation time. The rate equations for enzyme inactivation were determined using Equation 1.

$$k_{\text{obs}} = 0 + \frac{k_{\text{inact}} \cdot [I]}{K_I + [I]} \quad (1)$$

Where k_{obs} represents the observed rate of inactivation, k_{inact} (min^{-1}) is the maximum rate of inactivation, $[I]$ represents the time-dependent inhibitor concentration, and K_I is the concentration of time-dependent inhibitor that achieves one-half the maximum rate of inactivation. Kinetic parameters of CYP3A inactivation (k_{inact} and K_I) were determined by nonlinear regression of k_{obs} and nominal time-dependent inhibitor concentration using GraFit software (Version 7.0.2; Erithacus Software, Horley, Surrey, RH6 9YJ, UK). The reported apparent K_I values are estimates because the intracellular concentrations for each drug were not determined.

Clinical DDI predictions were determined for each of the time-dependent inhibitors using the input parameters from Table 1 and the corresponding in vitro inactivation kinetic parameters. AUC ratio (fold-change in midazolam AUC) was estimated using Equation 2 (Obach et al., 2006):

$$\frac{\text{AUC}_i}{\text{AUC}} = \frac{1}{F_g + \left((1 - F_g) \cdot \frac{1}{1 + \left(\frac{k_{\text{inact}} \cdot [I]_g}{k_{\text{deg,CYP3A,gut}} \cdot ([I]_g + K_I) \right)} \right)} \cdot \frac{1}{\left(\frac{f_{m(\text{CYP3A})}}{1 + \left(\frac{k_{\text{inact}} \cdot [I]_{\text{in vivo}}}{K_I \cdot k_{\text{deg,CYP3A,hep}}} \right)} \right) + (1 - f_{m(\text{CYP3A})})} \quad (2)$$

Where k_{inact} is the maximal rate of inactivation and K_I is the concentration of drug that yields 1/2-maximal rate of inactivation, $f_{m(\text{CYP3A})}$ is the fraction metabolized of selected substrate by CYP3A (midazolam, 0.93), F_g is the contribution of intestinal extraction (midazolam, 0.57), $[I]_{\text{in vivo}}$ is the free systemic concentration in vivo, and k_{deg} is the first order degradation rate constant of CYP3A

DMD #44644

hepatic (0.00032 min^{-1}) and CYP3A gut (0.00048 min^{-1}) (Greenblatt et al., 2003; Ghanbari et al., 2006).

The intestinal concentration of each of the time-dependent inhibitors was estimated using equation 3 (Obach et al., 2006):

$$[I]_g = \frac{D \cdot k_a \cdot F_a}{Q_g} \quad (3)$$

Where D is the dose administered, k_a is the absorption rate constant (0.03 min^{-1}), F_a is the fraction of the time-dependent inhibitor absorbed through the gut unchanged, and Q_g is human intestinal blood flow (248 ml/min). For a top limit estimate, each compound was assumed to be completely absorbed ($F_a = 1$). Human plasma protein binding values were used for estimating free systemic C_{\max} (Obach et al., 2006).

Results

Estimation of In Vitro Inactivation Parameters. Clarithromycin, mibefradil, verapamil, troleandomycin, and fluoxetine were incubated in a 150 donor pool of human liver microsomes for up to 30 minutes and in freshly plated hepatocytes, cryopreserved plated hepatocytes, and cryopreserved plated HepaRG for up to 30 minutes (fluoxetine up to 90 minutes), to determine pseudo first order rates of inactivation (k_{obs}). The apparent K_I and k_{inact} were then estimated from nonlinear regression of the k_{obs} determined for each time-dependent inhibitor concentration using Equation 1.

The apparent K_I and k_{inact} values obtained using HLMs were within the range of those previously published (Table 2). Mibefradil and troleandomycin both exhibited moderate to strong inactivation potential with apparent K_I values of 1.1 and 1.8 μM , respectively, and k_{inact} values of 0.7 and 0.31 min^{-1} , respectively. Clarithromycin and verapamil both exhibited weak to moderate inactivation potential with apparent K_I values of 17.7 and 8.9 μM , respectively, and k_{inact} values of 0.05 and 0.1 min^{-1} , respectively. Fluoxetine exhibited weak inactivation potential with an apparent K_I of 8.6 μM and a k_{inact} of 0.005 min^{-1} . Given the weak inactivation of fluoxetine in vitro, it has been our experience that this is often not reproducible (data not shown).

The K_I and k_{inact} values obtained using freshly plated hepatocytes are reported in Table 2. Mibefradil and troleandomycin both exhibited moderate to strong inactivation potential with apparent K_I values of 0.6 and 0.9 μM , respectively, and k_{inact} values of 0.1 min^{-1} . Clarithromycin and verapamil both exhibited weak to moderate inactivation potential with apparent K_I values of 12.6 μM and k_{inact} values of 0.06 and 0.14 min^{-1} , respectively. Fluoxetine exhibited weak inactivation potential with an apparent K_I value of 7.3 μM and a k_{inact} value of 0.03 min^{-1} .

DMD #44644

The apparent K_I and k_{inact} values obtained using plated cryopreserved hepatocytes are reported in Table 2. Mibefradil and troleandomycin both exhibited moderate to strong inactivation potential with apparent K_I values of 0.2 and 0.6 μM , respectively, and k_{inact} values of 0.28 and 0.08 min^{-1} , respectively. Clarithromycin and verapamil both exhibited weak to moderate inactivation potential with apparent K_I values of 8.1 and 1.9 μM , respectively, and k_{inact} values of 0.09 and 0.14 min^{-1} , respectively. Fluoxetine exhibited weak inactivation potential with an apparent K_I of 17.1 μM and a k_{inact} of 0.03 min^{-1} .

The apparent K_I and k_{inact} values obtained using plated HepaRG are reported in Table 2. Mibefradil and troleandomycin both exhibited moderate to strong inactivation potential with apparent K_I values of 1.1 and 2.2 μM , respectively, and k_{inact} values of 0.91 and 0.17 min^{-1} , respectively. Clarithromycin and verapamil both exhibited weak to moderate inactivation potential with apparent K_I values of 5.4 and 5.5 μM , respectively, and k_{inact} values of 0.08 and 0.12 min^{-1} , respectively. Fluoxetine exhibited weak inactivation potential with an apparent K_I of 35.7 μM and a k_{inact} value of 0.01 min^{-1} .

Prediction of DDIs. Clinical DDI predictions were determined for each of the time-dependent inhibitors using the input parameters from Table 1 and the corresponding in vitro inactivation kinetic parameters from Table 2. Fold-change in AUC of victim drug midazolam was calculated using Equation 2 (Obach et al., 2006).

Fluoxetine is a known weak CYP3A time-dependent inhibitor with generally a lack of reported clinical CYP3A DDI (Lam et al., 2003). After an oral dose of 20-60 mg q.d. for 12 days, the observed clinical AUC_i/AUC ratio was 0.8. All plated cell systems and HLMs agreed with the general lack of clinically observed DDI in humans following oral dosing with the object drug

DMD #44644

midazolam (Figure 2 and Table 3). However, only the plated cell systems exhibited measureable time-dependent loss of activity due to the longer preincubation times (Figure 3).

Verapamil has a reported clinical CYP3A-mediated DDI where following an oral dose of 80 mg t.i.d. for 2 days, the observed clinical AUC_i/AUC ratio was 3-4 (Backman et al., 1994). The predicted DDI for verapamil using inactivation kinetic parameters derived from HLM and freshly plated hepatocytes was favorable at ~4-fold, whereas in cryopreserved plated hepatocytes and plated HepaRG, DDI predictions were 10-fold and 5-fold, respectively. Overall, with the exception of cryopreserved plated hepatocytes, the plated cell systems agreed with the HLM data, and fairly closely predicted the clinically observed DDI for verapamil (Figure 4 and Table 3).

A reported clinical CYP3A-mediated DDI has also been reported for clarithromycin (Gorski et al., 1998). Following an oral dosing regimen of 500 mg b.i.d. for 7 days, the observed clinical AUC_i/AUC ratio was 5-8 (Table 3). The predicted DDI for verapamil using HLM TDI data was 5-fold, in freshly plated hepatocytes was 7-fold, in cryopreserved plated hepatocytes was 11-fold, and in cryopreserved plated HepaRG was 12-fold. The plated system in closest agreement with the HLM predicted and actual reported DDI was freshly plated hepatocytes, with predicted AUC ratio of 7 (Table 3). Meanwhile, DDI estimates derived from cryopreserved plated hepatocytes and cryopreserved plated HepaRG, which were ~2-fold higher than predictions from HLM, were within approximately 2-fold of the reported clinical DDI (Figure 5 and Table 3).

The reported clinical CYP3A-mediated DDI for mibefradil is ~9 following a single oral dose of 100 mg (Veronese et al., 2003). The predicted DDI for mibefradil using inactivation parameters derived from HLM was 12-fold, in freshly plated hepatocytes was 6-fold, in cryopreserved plated hepatocytes was 16-fold, and in cryopreserved plated HepaRG was 13-fold. The plated system in closest agreement with the HLM-derived DDI prediction of 12, was cryopreserved plated HepaRG

DMD #44644

(13-fold). Cryopreserved plated hepatocytes were within approximately 2-fold of the observed clinical DDI. Freshly plated hepatocytes underpredicted the observed clinical DDI, due to the especially low k_{inact} observed of 0.1 min^{-1} .

Troleandomycin has a reported clinical CYP3A DDI (Kharasch et al., 2004). Following a single oral dose of 500 mg, the observed clinical AUC_i/AUC ratio was 15. The predicted DDI for troleandomycin using inactivation kinetic parameters derived from HLM and each cell system was comparable, between 21-23-fold. Each of the plated cell systems tested agreed with the human liver microsomal predicted DDI and roughly agreed with the clinically reported DDI (Figure 7 and Table 3).

Donor Variability. To assess the effect of donor-to-donor variability on clinical DDI prediction, fresh plated primary hepatocytes from three different donors were incubated with mibefradil. The three donors exhibited measurable differences in the in vitro inactivation kinetics with apparent K_I values of 0.54, 0.77, and $1.6 \mu\text{M}$ and k_{inact} values of 0.1, 0.16, and 0.36 min^{-1} , for donors H1014, FHVL, and MHVL, respectively (Figure 8). However, the differences between in vitro kinetic parameters did not translate to a difference in the predicted clinical interaction between midazolam and mibefradil, as the estimated DDI values for all three donors ranged from 5.5- to 6.3-fold.

Discussion

The FDA has issued several guidance documents which outline the need to evaluate drug candidates for the potential to cause drug-drug interactions (US Department of Health and Human Services, 2006). Most importantly, these documents describe decision trees and recommendations for examining the propensity of a drug to cause time-dependent inhibition of cytochrome P450. Despite improvements in the *in vitro* assays that are used to predict clinical DDI (Obach et al., 2006; Grimm et al., 2009), unexpected drug-drug interactions still occur, which may be due to limitations of *in vitro* systems. The ideal *in vitro* system for comprehensively evaluating drug-drug interactions should theoretically be human hepatocytes (Zhao, 2008) given the full complement of metabolic clearance mechanisms. Even though the ability to conduct *in vitro* DDI studies has been demonstrated in human hepatocyte suspensions (Mao et al., 2011), there are limitations with the long term viability and enzymatic activity of the cells in suspension (Zhao, 2008). It has been demonstrated that human plated cell systems offer unique advantages over human cell suspensions for time-dependent inhibition studies (Li and Doshi, 2011). Thus, the primary goal of these studies was to evaluate a number of different plated cell systems for the ability to generate inactivation kinetic parameters for CYP3A, the most important drug-metabolizing enzyme with respect to characterized mechanism for DDI. Further, we investigated plated cell systems for the ability to identify drug candidates that exhibit weak time-dependent inhibition of CYP3A by conducting experiments with preincubation times greater than 30 minutes with fluoxetine, a reported weak time-dependent inhibitor of CYP3A.

Pooled human liver microsomes (HLMs) are commonly used for measuring the potential of a compound to cause time-dependent inhibition of cytochrome P450 enzymes (Grimm et al., 2009). Based on the general acceptance of using human liver microsomes for time-dependent inhibition

DMD #44644

studies and the importance of evaluating CYP3A inactivation, this system was used as the standard for comparison when evaluating the ability of each of the plated cell systems to predict clinical DDI for CYP3A. The advantages of using HLMs include availability, low cost, ease of use, and literature support for using time-dependent inhibition data derived from this system to estimate with measurable accuracy the magnitude of clinical DDIs (Obach et al., 2006; Obach et al., 2007). However, limitations with using HLMs include inconsistent results for weak time-dependent inhibitors such as fluoxetine (Figure 3). Our lab routinely encounters weak time-dependent inhibitors in the discovery setting and a preincubation time of greater than 30 minutes may enable improved rank-ordering of compounds due to greater dynamic range. However, due to enzyme thermal degradation, the preincubation time for HLMs is generally limited to 30 minutes (Foti and Fisher, 2004). In addition, the inability to assess non-CYP mediated mechanisms (unless costly co-factors are added) is a limitation associated with the use of the HLM fraction.

Sandwich-cultured fresh plated hepatocytes are commonly used for cytochrome P450 induction assessment. As such, this system was chosen to be evaluated for the ability to assess TDI of CYP3A. One of the main challenges associated with the use of freshly plated primary hepatocytes is the donor-to-donor variability and limited availability. Several donors were tested over a time span of approximately one year to determine the inactivation kinetic parameters of the five tested time-dependent inhibitors. The longer duration of the testing was due to the limited availability of cells from human donors with acceptable demographics and CYP3A activity. During the course of this study our lab observed substantial donor-to-donor variability in CYP3A activity (data not shown), consistent with literature reports (Moore and Gould, 1984). In addition, the cost of purchasing the plated hepatocytes is substantially higher than using human liver microsomes. The advantages of using freshly plated hepatocytes are general ease of use due to the

DMD #44644

ability to purchase cells pre-plated in sandwich culture and the ability to assess non-CYP mediated mechanism due to the presence of a full complement of drug metabolizing enzymes. Although the inactivation kinetic parameters derived from freshly plated human hepatocytes generally agreed with human liver microsomal parameters (Table 2) and the reported clinical DDI (Table 3), taking into consideration the limited availability of fresh primary human hepatocytes, this in vitro system may not be suitable for routine screening of compounds for CYP3A TDI, but may serve as a suitable in vitro system for more definitive assessment of CYP3A TDI, similar to the current approaches for assessing cytochrome P450 induction liabilities.

Cryopreserved hepatocytes are commonly used to assess the in vitro metabolic clearance of pharmaceutical compounds. FDA guidance also establishes plateable cryopreserved hepatocytes as an acceptable model for assessment of human cytochrome P450 induction. The advantages of using cryopreserved plated hepatocytes include availability of cells from multiple donors and the ability to assess non-CYP clearance mechanisms due to the presence of a full complement of hepatic drug metabolizing enzymes. Interestingly, the apparent K_I for mibefradil and verapamil tested in this system was generally 5- to 6-fold lower than the apparent K_I derived in HLM and fresh plated systems (Table 2). This decrease in apparent K_I translates to an overprediction compared to the reported pharmacokinetic CYP3A DDI (Table 3). It is unclear why this difference was observed. The main limitations with using cryopreserved hepatocytes are the overall cost for a plateable lot of cells, as well as the plating process which requires an overlay.

The HepaRG cell line has been reported to be useful for assessing cytochrome P450 induction and other human drug metabolism studies based on previously published studies (Le Vee et al., 2006; Kanebratt and Andersson, 2008b). The advantages of using cryopreserved plated HepaRG are general ease of use due to good cell viability, simple plating procedure, acceptable expression

DMD #44644

levels of CYP3A (Kanebratt and Andersson, 2008a), and an unlimited supply of the same cell line, which would circumvent the need to recharacterize new lots of cryopreserved hepatocytes for CYP3A activity. Unlike human liver microsomes, where weak fluoxetine inactivation kinetics may be difficult to consistently reproduce due to limitations with the length of preincubation time, we were easily able to detect the weak CYP3A inactivation using cryopreserved plated HepaRG cells (Figure 3), which suggests that this in vitro system may be suitable for this challenging task. However, one should understand that the expression levels of certain drug metabolizing enzymes, such as CYP2D6, are lower than desired, which may limit the utility of the cell line for evaluating TDI of additional CYP enzymes (Kanebratt and Andersson, 2008a).

In summary, freshly plated hepatocytes appear to provide clinical DDI estimates that are roughly equivalent to human liver microsomes and approximate those observed clinically. However, given the evidence for potential donor to donor variability and infrequent availability, this system is not a viable choice for routine assessment of time-dependent inhibition in a discovery setting. In addition, use of cryopreserved hepatocytes, while also demonstrated as useful for characterizing CYP3A time-dependent inhibitors, is fraught with potential issues such as cost, and the need to re-characterize new lots of cells. Overall, the HepaRG cell model appears to be a suitable system for an early assessment of time-dependent inhibition of CYP3A in the discovery setting, although further characterization for their utility of assessing TDI of additional P450 enzymes needs to be conducted. Data reported here should provide a benchmark for determined inactivation kinetic parameters and predicted clinical DDI for CYP3A time-dependent inhibitors using the cryopreserved plated HepaRG cell system. Now that we have conducted a baseline assessment for the ability to characterize well-known time-dependent inhibitors in these cell models, future activities in our lab will focus on evaluating non-CYP mediated mechanisms of

DMD #44644

time-dependent inhibition using plated cell systems, such as those reported with gemfibrozil (Ogilvie et al., 2006).

DMD #44644

Acknowledgements. We thank Dr. Dustin Smith (Boehringer-Ingelheim Pharmaceuticals) for carefully reviewing the manuscript and providing valuable comments and David Joseph (Boehringer-Ingelheim Pharmaceuticals) for his valuable advice and suggestions regarding assessment of TDI in freshly plated hepatocytes. Finally, Dr. Jonathon Jackson (Life Technologies) for his expert advice regarding plating and maintenance of HepaRG cells and cryopreserved hepatocytes.

DMD #44644

Authorship Contributions

Participated in research design: Daniel R. Albaugh, Michael B. Fisher, Cody L. Fullenwider, J.

Matthew Hutzler

Conducted experiments: Daniel R. Albaugh, Cody L. Fullenwider

Contributed new reagents or analytic tools: Daniel R. Albaugh, Cody L. Fullenwider

Performed data analysis: Daniel R. Albaugh, Cody L. Fullenwider, J. Matthew Hutzler

Wrote or contributed to the writing of the manuscript: Daniel R. Albaugh, Michael B. Fisher, Cody

L. Fullenwider, and J. Matthew Hutzler

References

- Backman JT, Olkkola KT, Aranko K, Himberg JJ, and Neuvonen PJ (1994) Dose of midazolam should be reduced during diltiazem and verapamil treatments. *Br J Clin Pharmacol* **37**:221-225.
- Baer BR, DeLisle RK, and Allen A (2009) Benzylic oxidation of gemfibrozil-1-O-beta-glucuronide by P450 2C8 leads to heme alkylation and irreversible inhibition. *Chem Res Toxicol* **22**:1298-1309.
- Correia MA (1991) Cytochrome P450 turnover. *Methods Enzymol* **206**:315-325.
- Foti RS and Fisher MB (2004) Impact of incubation conditions on bufuralol human clearance predictions: enzyme lability and nonspecific binding. *Drug Metab Dispos* **32**:295-304.
- Ghanbari F, Rowland-Yeo K, Bloomer JC, Clarke SE, Lennard MS, Tucker GT, and Rostami-Hodjegan A (2006) A critical evaluation of the experimental design of studies of mechanism based enzyme inhibition, with implications for in vitro-in vivo extrapolation. *Curr Drug Metab* **7**:315-334.
- Gorski JC, Jones DR, Haehner-Daniels BD, Hamman MA, O'Mara EM, Jr., and Hall SD (1998) The contribution of intestinal and hepatic CYP3A to the interaction between midazolam and clarithromycin. *Clin Pharmacol Ther* **64**:133-143.
- Greenblatt DJ, von Moltke LL, Harmatz JS, Chen G, Weemhoff JL, Jen C, Kelley CJ, LeDuc BW, and Zinny MA (2003) Time course of recovery of cytochrome p450 3A function after single doses of grapefruit juice. *Clin Pharmacol Ther* **74**:121-129.
- Grimm SW, Einolf HJ, Hall SD, He K, Lim HK, Ling KH, Lu C, Nomeir AA, Seibert E, Skordos KW, Tonn GR, Van Horn R, Wang RW, Wong YN, Yang TJ, and Obach RS (2009) The conduct of in vitro studies to address time-dependent inhibition of drug-metabolizing

DMD #44644

enzymes: a perspective of the pharmaceutical research and manufacturers of America.

Drug Metab Dispos **37**:1355-1370.

Honkalammi J, Niemi M, Neuvonen PJ, and Backman JT (2011) Mechanism-based inactivation of

CYP2C8 by gemfibrozil occurs rapidly in humans. *Clin Pharmacol Ther* **89**:579-586.

Jones DR, Gorski JC, Hamman MA, Mayhew BS, Rider S, and Hall SD (1999) Diltiazem

inhibition of cytochrome P-450 3A activity is due to metabolite intermediate complex formation. *J Pharmacol Exp Ther* **290**:1116-1125.

Kanebratt KP and Andersson TB (2008a) Evaluation of HepaRG cells as an in vitro model for

human drug metabolism studies. *Drug Metab Dispos* **36**:1444-1452.

Kanebratt KP and Andersson TB (2008b) HepaRG cells as an in vitro model for evaluation of

cytochrome P450 induction in humans. *Drug Metab Dispos* **36**:137-145.

Kharasch ED, Walker A, Hoffer C, and Sheffels P (2004) Intravenous and oral alfentanil as in vivo

probes for hepatic and first-pass cytochrome P450 3A activity: noninvasive assessment by use of pupillary miosis. *Clin Pharmacol Ther* **76**:452-466.

Lam YW, Alfaro CL, Ereshefsky L, and Miller M (2003) Pharmacokinetic and pharmacodynamic

interactions of oral midazolam with ketoconazole, fluoxetine, fluvoxamine, and nefazodone. *J Clin Pharmacol* **43**:1274-1282.

Le Vee M, Jigorel E, Glaise D, Gripon P, Guguen-Guillouzo C, and Fardel O (2006) Functional

expression of sinusoidal and canalicular hepatic drug transporters in the differentiated human hepatoma HepaRG cell line. *Eur J Pharm Sci* **28**:109-117.

Li AP (1997) Primary hepatocyte cultures as an in vitro experimental model for the evaluation of

pharmacokinetic drug-drug interactions. *Adv Pharmacol* **43**:103-130.

DMD #44644

- Li AP and Doshi U (2011) Higher Throughput Human Hepatocyte Assays for the Evaluation of Time-Dependent Inhibition of CYP3A4. *Drug Metab Lett* **5**:183-191.
- Lin JH and Lu AY (1998) Inhibition and induction of cytochrome P450 and the clinical implications. *Clin Pharmacokinet* **35**:361-390.
- Lu C, Berg C, Prakash SR, Lee FW, and Balani SK (2008a) Prediction of pharmacokinetic drug-drug interactions using human hepatocyte suspension in plasma and cytochrome P450 phenotypic data. III. In vitro-in vivo correlation with fluconazole. *Drug Metab Dispos* **36**:1261-1266.
- Lu C, Hatsis P, Berg C, Lee FW, and Balani SK (2008b) Prediction of pharmacokinetic drug-drug interactions using human hepatocyte suspension in plasma and cytochrome P450 phenotypic data. II. In vitro-in vivo correlation with ketoconazole. *Drug Metab Dispos* **36**:1255-1260.
- Mao J, Mohutsky MA, Harrelson JP, Wrighton SA, and Hall SD (2011) Prediction of CYP3A-mediated drug-drug interactions using human hepatocytes suspended in human plasma. *Drug Metab Dispos* **39**:591-602.
- Mayhew BS, Jones DR, and Hall SD (2000) An in vitro model for predicting in vivo inhibition of cytochrome P450 3A4 by metabolic intermediate complex formation. *Drug Metab Dispos* **28**:1031-1037.
- McGinnity DF, Berry AJ, Kenny JR, Grime K, and Riley RJ (2006) Evaluation of time-dependent cytochrome P450 inhibition using cultured human hepatocytes. *Drug Metab Dispos* **34**:1291-1300.
- Moore CJ and Gould MN (1984) Metabolism of benzo[a]pyrene by cultured human hepatocytes from multiple donors. *Carcinogenesis* **5**:1577-1582.

DMD #44644

- Obach RS, Walsky RL, and Venkatakrishnan K (2007) Mechanism-based inactivation of human cytochrome p450 enzymes and the prediction of drug-drug interactions. *Drug Metab Dispos* **35**:246-255.
- Obach RS, Walsky RL, Venkatakrishnan K, Gaman EA, Houston JB, and Tremaine LM (2006) The utility of in vitro cytochrome P450 inhibition data in the prediction of drug-drug interactions. *J Pharmacol Exp Ther* **316**:336-348.
- Ogilvie BW, Zhang D, Li W, Rodrigues AD, Gipson AE, Holsapple J, Toren P, and Parkinson A (2006) Glucuronidation converts gemfibrozil to a potent, metabolism-dependent inhibitor of CYP2C8: implications for drug-drug interactions. *Drug Metab Dispos* **34**:191-197.
- US Department of Health and Human Services FaDA (2006) Drug Interaction Studies-Study design, data analysis, and recommendations for dosing and labeling.
- Van LM, Swales J, Hammond C, Wilson C, Hargreaves JA, and Rostami-Hodjegan A (2007) Kinetics of the time-dependent inactivation of CYP2D6 in cryopreserved human hepatocytes by methylenedioxymethamphetamine (MDMA). *Eur J Pharm Sci* **31**:53-61.
- Veronese ML, Gillen LP, Dorval EP, Hauck WW, Waldman SA, and Greenberg HE (2003) Effect of mibefradil on CYP3A4 in vivo. *J Clin Pharmacol* **43**:1091-1100.
- Wandel C, Kim RB, Guengerich FP, and Wood AJ (2000) Mibefradil is a P-glycoprotein substrate and a potent inhibitor of both P-glycoprotein and CYP3A in vitro. *Drug Metab Dispos* **28**:895-898.
- Welker HA (1998) Single- and multiple-dose mibefradil pharmacokinetics in normal and hypertensive subjects. *J Pharm Pharmacol* **50**:983-987.

DMD #44644

Xu L, Chen Y, Pan Y, Skiles GL, and Shou M (2009) Prediction of human drug-drug interactions from time-dependent inactivation of CYP3A4 in primary hepatocytes using a population-based simulator. *Drug Metab Dispos* **37**:2330-2339.

Zhao P (2008) The use of hepatocytes in evaluating time-dependent inactivation of P450 in vivo. *Expert Opin Drug Metab Toxicol* **4**:151-164.

Zhao P, Kunze KL, and Lee CA (2005) Evaluation of time-dependent inactivation of CYP3A in cryopreserved human hepatocytes. *Drug Metab Dispos* **33**:853-861.

Zhao P, Lee CA, and Kunze KL (2007) Sequential metabolism is responsible for diltiazem-induced time-dependent loss of CYP3A. *Drug Metab Dispos* **35**:704-712.

DMD #44644

Footnotes

Reprint requests to:

Daniel Albaugh

Boehringer-Ingelheim Pharmaceuticals Inc., Medicinal Chemistry (DMPK)

175 Briar Ridge Road, R&D 10578, Ridgefield, CT 06877

Email: daniel.albaugh@boehringer-ingelheim.com

Legends for Figures

Figure 1. Chemical structures of CYP3A time-dependent inhibitors.

Figure 2. Kinetic plots (K_{obs} vs. time-dependent inhibitor concentration) illustrating time-dependent loss of CYP3A activity with fluoxetine in (A) human liver microsomes, (B) freshly plated hepatocytes, (C) cryopreserved plated hepatocytes, and (D) cryopreserved plated HepaRG.

Figure 3. Semi-logarithmic plots (LN % activity remaining vs. incubation time) illustrating the time-dependent loss of enzymatic activity in (A) human liver microsomes and (B) cryopreserved plated HepaRG with the weak CYP3A time-dependent inhibitor fluoxetine.

Figure 4. Kinetic plots (K_{obs} vs. time-dependent inhibitor concentration) illustrating time-dependent loss of CYP3A activity with verapamil in (A) human liver microsomes, (B) freshly plated hepatocytes, (C) cryopreserved plated hepatocytes, and (D) cryopreserved plated HepaRG.

Figure 5. Kinetic plots (K_{obs} vs. time-dependent inhibitor concentration) illustrating time-dependent loss of CYP3A activity with clarithromycin in (A) human liver microsomes, (B) freshly plated hepatocytes, (C) cryopreserved plated hepatocytes, and (D) cryopreserved plated HepaRG.

Figure 6. Kinetic plots (K_{obs} vs. time-dependent inhibitor concentration) illustrating time-dependent loss of CYP3A activity with mibefradil in (A) human liver microsomes, (B) freshly plated hepatocytes, (C) cryopreserved plated hepatocytes, and (D) cryopreserved plated HepaRG.

Figure 7. Kinetic plots (K_{obs} vs. time-dependent inhibitor concentration) illustrating time-dependent loss of CYP3A activity with troleandomycin in (A) human liver microsomes, (B) freshly plated hepatocytes, (C) cryopreserved plated hepatocytes, and (D) cryopreserved plated HepaRG.

DMD #44644

Figure 8. Kinetic plots (K_{obs} vs. time-dependent inhibitor concentration) illustrating time-dependent loss of CYP3A activity with mibefradil in freshly plated human hepatocytes with (A) Lot H1014, (B) Lot FHVL, and (C) Lot MHVL demonstrating the effect of donor variability.

TABLE 1. Summary of published data utilized for the prediction of clinical drug-drug interaction for each of the tested CYP3A time-dependent inhibitors.

Parameter	Clarithromycin	Mibefradil	Troleandomycin	Verapamil	Fluoxetine
Dose	500 mg	100 mg	500 mg	80 mg	20-60 mg
Interval	b.i.d. (7 days)	Single Dose	Single Dose	t.i.d. (2 days)	q.d. (12 days)
MW ^a	747.95	495.63	813.97	454.60	309.33
C _{sys} ^b	673 ng/mL	520 ng/mL ^c	2000 ng/mL ^d	157 ng/mL	115 ng/mL
f _u ^e	0.3	0.005	0.15	0.1	0.05
C _{sys, u} ^f	202 ng/mL	2.6 ng/mL	300 ng/mL	15.7 ng/mL	5.75 ng/mL
Reference	(Gorski et al., 1998)	(Veronese et al., 2003)	(Kharasch et al., 2004)	(Backman et al., 1994)	(Lam et al., 2003)

a Molecular weight

b Systemic concentration (C_{max})

c Information from Welker et al. (Welker, 1998)

d Information from the University of Washington Metabolism and Transport Drug Interaction Database (2011, <http://www.druginteractioninfo.org>)

e Fraction of unbound drug. Values taken from Obach et al. (Obach et al., 2006)

f Free systemic concentration (C_{max})

DMD #44644

TABLE 2. Kinetic parameters of CYP3A time-dependent inhibitors

Compound	Fresh ^a		Cryopreserved ^b		HepaRG ^c		HLM ^d	
	K_I	k_{inact}	K_I	k_{inact}	K_I	k_{inact}	K_I	k_{inact}
	(μM)	(min^{-1})	(μM)	(min^{-1})	(μM)	(min^{-1})	(μM)	(min^{-1})
Clarithromycin	12.6	0.06	8.1	0.09	5.4	0.08	17.7	0.05
Mibefradil	0.6	0.10	0.2	0.28	1.1	0.91	1.1	0.70
Troleandomycin	0.9	0.10	0.6	0.08	2.2	0.17	1.8	0.31
Verapamil	12.6	0.14	1.9	0.14	5.5	0.12	8.9	0.10
Fluoxetine	7.3	0.03	17.1	0.03	35.7	0.01	8.6	0.005

- a Freshly plated human hepatocytes
 b Cryopreserved plated human hepatocytes
 c Cryopreserved plated HepaRG
 d Human liver microsomes

DMD #44644

TABLE 3. Comparison of predicted clinical drug-drug interactions (fold-change in AUC with object drug midazolam) from in vitro kinetic parameters of CYP3A time-dependent inhibitors

Model	Clarithromycin	Mibefradil	Troleandomycin	Verapamil	Fluoxetine
Range of Clinical DDI	5-8	9	15	3-4	No interaction
Reference	(Gorski et al., 1998)	(Veronese et al., 2003)	(Kharasch et al., 2004)	(Backman et al., 1994)	(Lam et al., 2003)
HLM ^a	5	12	23	4	2
FreshHep ^b	7	6	22	4	2
CryoHep ^c	11	16	22	10	2
HepaRG ^d	12	13	21	5	2

a Human liver microsomes

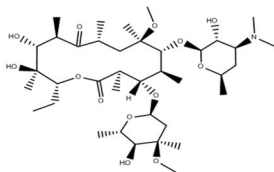
b Freshly plated human hepatocytes

c Cryopreserved plated human hepatocytes

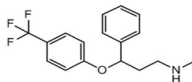
d Cryopreserved plated HepaRG

note Predicted fold-change in AUC calculated using equation 2

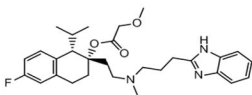
Figure 1



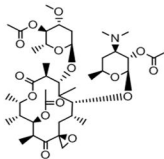
Clarithromycin



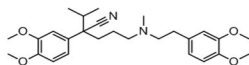
Fluoxetine



Mibefradil



Troleandomycin



Verapamil

Figure 2

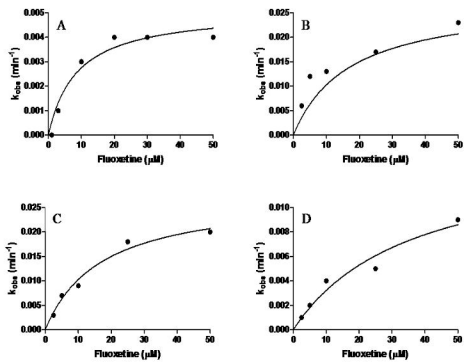


Figure 3

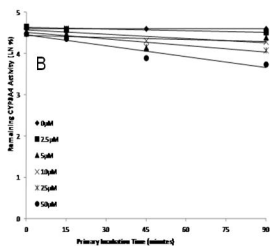
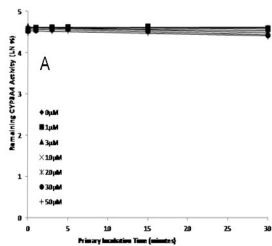


Figure 4

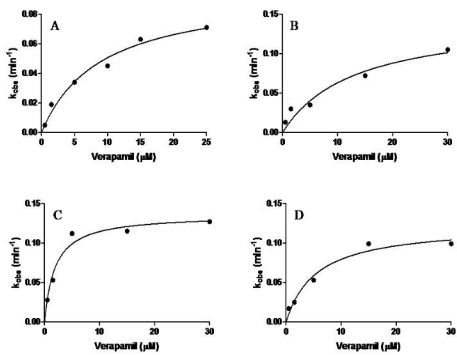


Figure 5

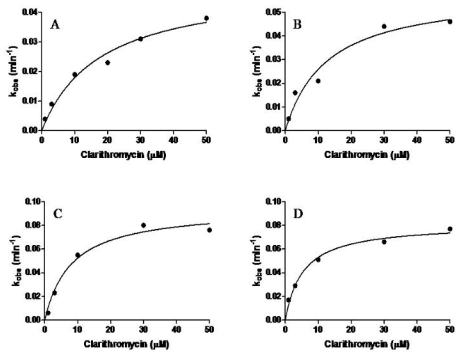


Figure 6

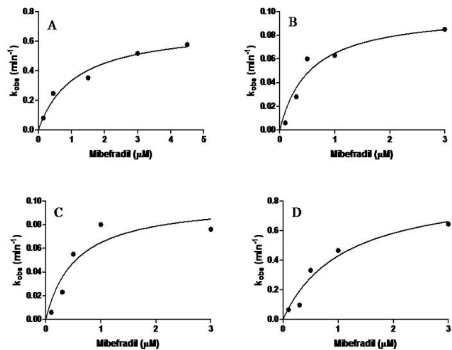


Figure 7

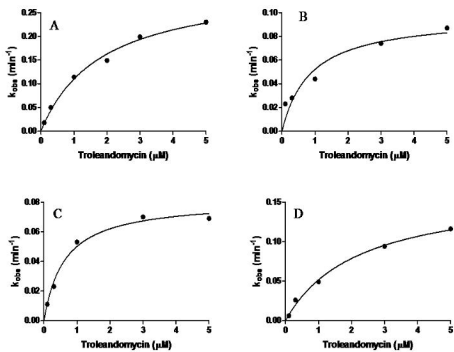


Figure 8

